HHS Public Access

Author manuscript

*Kidney Int*. Author manuscript; available in PMC 2026 February 02.

Published in final edited form as:

*Kidney Int*. 2024 July ; 106(1): 98–114. doi:10.1016/j.kint.2024.02.023.

# Hypermethylation leads to the loss of HOXA5, resulting in JAG1 expression and NOTCH signaling contributing to kidney fibrosis

**Xiao Xiao**[1,7], **Wei Wang**[2,7], **Chunyuan Guo**[3,7], **Jiazhu Wu**[4], **Sheng Zhang**[5], **Huidong Shi**[6], **Sangho Kwon**[7], **Jiankang Chen**[7], **Zheng Dong**[8]

[1]Department of Laboratory Medicine, Zhongnan Hospital of Wuhan University, Wuhan, China

[2]Department of Urology, Institute of Urology, and Anhui Province Key Laboratory of Genitourinary Diseases, the First Affiliated Hospital of Anhui Medical University, Hefei, China

[3]Department of Dermatology, Shanghai Skin Disease Hospital, and Institute of Psoriasis, Tongji University School of Medicine, Shanghai, China

[4]Department of Hematology, the First Affiliated Hospital of Nanjing Medical University, Nanjing, China

[5]Department of Spine Surgery and Musculoskeletal Tumor, Zhongnan Hospital of Wuhan University, Wuhan, China

[6]Cancer Center, Medical College of Georgia at Augusta University, Augusta, Georgia, USA

[7]Department of Cellular Biology and Anatomy, Medical College of Georgia at Augusta University, Augusta, Georgia, USA

[8]Department of Cellular Biology and Anatomy, Medical College of Georgia at Augusta University and Charlie Norwood VA Medical Center, Augusta, Georgia, USA

## Abstract

Epigenetic regulations, including DNA methylation, are critical to the development and progression of kidney fibrosis, but the underlying mechanisms remain elusive. Here, we show that fibrosis of the mouse kidney was associated with the induction of DNA methyltransferases and increases in global DNA methylation and was alleviated by the DNA methyltransferase inhibitor 5-Aza-2′-deoxycytidine (5-Aza). Genome-wide analysis demonstrated the hypermethylation of 94 genes in mouse unilateral ureteral obstruction kidneys, which was markedly reduced by 5-Aza. Among these genes, *Hoxa5* was hypermethylated at its gene promoter, and this hypermethylation was associated with reduced HOXA5 expression in fibrotic mouse kidneys after ureteral obstruction or unilateral ischemia-reperfusion injury. 5-Aza prevented *Hoxa5* hypermethylation, restored HOXA5 expression, and suppressed kidney fibrosis. Downregulation of HOXA5 was



**Correspondence:** Zheng Dong, Department of Cellular Biology and Anatomy, Medical College of Georgia at Augusta University and Charlie Norwood VA Medical Center, 1640 Laney Walker Boulevard, CB 1124, Augusta, Georgia 30912, USA. zdong@augusta.edu; or Xiao Xiao, Department of Laboratory Medicine, Zhongnan Hospital of Wuhan University, 169 Donghu Road, Wuhan 430071, China. xiaox1017@whu.edu.cn.

DISCLOSURE

All the authors declared no competing interests.

verified in human kidney biopsies from patients with chronic kidney disease and correlated with the increased kidney fibrosis and DNA methylation. Kidney fibrosis was aggravated by conditional knockout of *Hoxa5* and alleviated by conditional knockin of *Hoxa5* in kidney proximal tubules of mice. Mechanistically, we found that HOXA5 repressed *Jag1* transcription by directly binding to its gene promoter, resulting in the suppression of JAG1-NOTCH signaling during kidney fibrosis. Thus, our results indicate that loss of HOXA5 via DNA methylation contributes to fibrogenesis in kidney diseases by inducing JAG1 and consequent activation of the NOTCH signaling pathway.

**Keywords**

DNA methylation; HOXA5; JAG1; kidney fibrosis; NOTCH signaling

Chronic kidney disease (CKD) is a major public health problem with a growing burden of complications, associated morbidity, and mortality globally.[1–4] Kidney fibrosis is a common pathologic feature of CKD that develops through tubular degeneration, inflammation, interstitial fibroblast activation, and deposition of extracellular matrix proteins to replace the functional parenchyma, ultimately leading to kidney dysfunction.[5,6] Despite critical clinical needs and extensive research, the understanding of kidney fibrosis regulation remains limited. Therefore, an in-depth exploration of the molecular mechanism of renal fibrosis is beneficial to discovering biomarkers and treating the disease.

DNA methylation is a common epigenetic modification that regulates gene expression without altering primary nuclear acid sequences. DNA methylation is involved in various kidney diseases, including acute kidney injury, diabetic nephropathy, hypertension nephropathy, graft rejection, and kidney tumors.[7–16] In the context of CKD, genome-wide cytosine methylation in human kidney tubular cells is positively correlated with kidney fibrosis and is a useful biomarker for diabetic kidney disease.[12] Scattered studies reported the effects of DNA methylation inhibitors (eg, 5-aza-2′-deoxycytidine or 5-Aza) or activators (eg, hydralazine) on kidney fibrosis, but they did not reach a consistent conclusion.[17–20]

Recent application of sequencing technology led to the identification of numerous differential DNA methylation regions (DMRs) that distribute across multiple genetic loci, providing significant new insights. However, most genes with aberrant DNA methylation modifications have not been characterized. *HOXA5* is one of A cluster-Homeobox genes encoding the Homeobox a5 protein (HOXA5), which is a highly conserved transcriptional factor that participates in DNA synthesis, cell differentiation, and organ development.[21,22] Previous studies have demonstrated that promoter hypermethylation of *HOXA5* is linked to multiple pathologies, such as clear cell renal cell carcinoma[23] and chronic obstructive pneumonia disease.[24] However, the role of HOXA5 in kidney diseases including renal fibrosis is largely unknown.

JAG1 is a critical ligand of the NOTCH signaling pathway that mediates cell differentiation, proliferation, and lineage specification through cell-to-cell communication. NOTCH signaling is critical in organ development, and, not surprisingly, protein levels in the NOTCH signaling pathway are suppressed and stationary once organ development is

completed,[25] whereas aberrantly elevated JAG1 may stimulate canonical NOTCH signaling and promote fibrosis in various organs.[26–29]

In this study, we demonstrated that HOXA5 was hypermethylated at its gene promoter during kidney fibrosis, resulting in a loss of expression, which contributed significantly to kidney fibrosis. HOXA5 represses *Jag1* transcription and associates with NOTCH signaling. Together, these results indicate that loss of *HOXA5* due to hypermethylation contributes to kidney fibrogenesis by inducing JAG1 for the activation of NOTCH signaling.

## METHODS

### Animals

C57BL/6J mice were purchased from the Jackson Laboratory and maintained in the animal facility of Charlie Norwood VA Medical Center (Augusta, GA), or purchased from and maintained in the Center of Disease Prevention and Control of Hubei province (Wuhan, China). *Hoxa5*-floxed mice were initially generated by GemPharmatech Co., Ltd. Transgenic mice were maintained under a 12-hour light/12-hour dark cycle with free access to food and water in the animal facility of Wuhan University. The details of transgenic mice were described in the Supplementary Methods.

### Primary cell isolation

Primary proximal tubular cells were isolated from 3-week-old $Hoxa5^{ptCKO}$ mice and $Hoxa5^{ptCKI}$ mice. Briefly, kidney cortex tissues were minced and digested with collagenase type IV (2091MG100; BioFroxx). Proximal tubular cells were then purified by centrifugation at 2000 *g* in isolation medium containing 32% percoll (P8370; Solarbio) and cultured in culture medium (CM-M062; Procell) supplemented with 10% fetal bovine serum (Gibco). After 6 days of growth, the first passage of primary tubular cells was digested and seeded in 35 mm dishes at $0.3 \times 10^6$ cells/dish. The next day cells were infected with adenovirus expressing green fluorescent protein or adenovirus expressing Cre-green fluorescent protein (AP23051601; HANBIO). Twenty-four hours after infection, the cells were incubated in culture medium with 2% fetal bovine serum overnight followed by treatment with saline or 10 ng/ml transforming growth factor (TGF)-β1 for 72 hours.

### Human kidney biopsy

Paraffin-embedded human kidney tissue samples were obtained from the Department of Pathology at Zhongnan Hospital of Wuhan University (Wuhan, China). The fibrotic biopsies were from patients diagnosed with CKD, including chronic nephritis, diabetic nephropathy, and hypertensive nephropathy. The control biopsies were the normal, distant paracarcinoma tissues dissected from patients with renal cancer. Kidney specimens without cortical parts were excluded from this study. Finally, a total of 10 CKD specimens and 8 normal (control) specimens were analyzed.

### Statistical analysis

Results were represented as the mean ± SEM using Prism 8 (GraphPad). Differences between multiple groups were analyzed using 1-way analysis of variance, and differences

between the 2 groups were compared with a 2-tailed Student's *t* test. Differences are significant when $P < 0.05$.

### Study approval

This study was approved by the Ethics Committee of the Zhongnan Hospital of Wuhan University, Wuhan, China. Animal studies were approved by the Institutional Animal Care and Use Committees of Charlie Norwood Veterans Affairs Medical Center (Augusta, Georgia) and Zhongnan Hospital of Wuhan University (Wuhan, China).

Primers for polymerase chain reaction are listed in Supplementary Tables S1–S3. Additional details for methods are provided in the Supplementary Methods.

## RESULTS

### Kidney fibrosis is associated with DNA methylation and is suppressed by inhibitors of DNA methyltransferases

To determine the role of DNA methylation in kidney fibrosis, we first examined the expression of DNA methyltransferases in the kidney following the mouse unilateral ureter obstruction (UUO) model. DNMT1, DNMT3a, and DNMT3b were induced by UUO, which was blocked by the DNMT inhibitor 5-Aza (Figure 1a–d). Consistently, DNA methylation, shown by 5′-methylcytosine (5mC) staining, was markedly induced in UUO kidneys, and this induction was diminished by 5-Aza (Figure 1e). Because 5mC modification occurs in both DNA and RNA,[30] we performed a dot blot experiment to specifically analyze 5mC modification in RNA. The level of 5mC in the RNA sample from UUO tissues did not differ from that in sham-controlled kidney tissues (Supplementary Figure S1), indicating that the increase in 5mC modification in UUO kidneys was mainly due to DNA methylation. Notably, 5-Aza attenuated kidney fibrosis during UUO as indicated by reduced expression of fibrosis marker proteins, such as fibronectin and α-smooth muscle actin (α-SMA) (Figure 1f–h), and decreased collagen deposition as shown by Masson's trichrome staining (Figure 1i and j).

We further tested the effect of 5-Aza on kidney fibrosis after unilateral ischemia-reperfusion injury (UIRI). 5-Aza was given 2 days after UIRI to collect samples on day 14 for analysis (Supplementary Figure S2A). The UIRI kidney showed a functional decline as indicated by blood urea nitrogen and serum creatine increases and the induction of DNMT1 and fibrosis marker proteins. These changes were partially ameliorated by 5-Aza (Supplementary Figure S2B–G). Collectively, DNA methylation is induced in, and contribute to, kidney fibrosis in both UUO and UIRI models.

### Profiling of DNA methylation in UUO kidneys

To discover genes with aberrant DNA methylation in kidney fibrosis, we analyzed profiled DNA methylation changes by reduced representation bisulfite sequencing. The heatmaps showed an overall increase in DNA methylation in UUO kidney tissues compared with control, which was normalized by 5-Aza as expected (Figure 2a). Analysis of DMRs revealed that most DMRs were in the coding regions or intergenic areas of genes. In total,

9.7% and 7.7% of DMRs were found in the promoter region when comparing UUO with sham and UUO with 5-Aza groups, respectively (Figure 2b).

In comparison with the sham control, UUO induced 165 hypermethylated DMRs and 27 hypomethylated DMRs. Corresponding to these DMRs, 234 genes were hypermethylated and 39 genes were hypomethylated in UUO kidneys, compared with the sham control. 5-Aza suppressed DNA methylation in UUO, resulting in 362 hypomethylated DMRs and only 4 hypermethylated DMRs, which corresponded to hypomethylation in 547 genes and hypermethylation in only 8 genes (Supplementary Tables S4–S7).

## Promoter methylation of *Hoxa5* is associated with renal fibrosis in UUO and UIRI

In reduced representation bisulfite sequencing analysis, 94 genes were hypermethylated in UUO, and their methylation was diminished by 5-Aza (Figure 3a; Supplementary Table S8). A major epigenetic mechanism of DNA methylation is the hypermethylation of gene promoters that leads to the suppression of target gene transcription.[7,12,31] In the identified 94 genes, only 5 had promoter hypermethylation in UUO that was suppressed by 5-Aza, namely *A930004D18Rik*, *6330409D20Rik*, *Pds5b*, *Hoxa5*, and *AI428936* (Figure 3a). Interestingly, of these 5 genes, only *Hoxa5* showed a negative correlation between transcription and promoter methylation. In light of this, we focused on *Hoxa5* for further investigation.

The *Hoxa5* promoter contains a DMR with 7 CpG sites (Figure 3b). Each of these 7 CpG sites was methylated more during UUO, and 5-Aza reduced this increase. To validate the reduced representation bisulfite sequencing results, we quantified the *Hoxa5* promoter methylation level by pyrosequencing. As shown in Figure 3d, pyrosequencing confirmed that UUO significantly increased DNA methylation on the *Hoxa5* promoter (*P* value was 0.0130), and this increase was attenuated by 5-Aza significantly (*P* value was 0.0149). Similar hypermethylation was observed in kidney cortex tissues after UIRI, which was suppressed by 5-Aza (Supplementary Figure S3A).

## HOXA5 is expressed in tubular cells and its expression is regulated by DNA methylation

To study the regulation of HOXA5 by DNA methylation in renal fibrosis, we first localized its expression in mouse kidney tissues. Co-staining of HOXA5 and specific kidney cell markers indicated that HOXA5 was mainly expressed in aquaporin 1–positive proximal tubular cells (Figure 4a). Some distal tubules with kidney-specific cadherin-positive staining also had HOXA5 nuclear staining. In contrast, HOXA5 staining was detected in very few α-SMA-expressing fibroblasts and aquaporin 2–positive collecting tubule cells and not F4/80-positive macrophages (Figure 4a).

We then analyzed HOXA5 expression during renal fibrosis. UUO and UIRI led to a significant decrease in HOXA5 expression, which was prevented by 5-Aza (Figure 4b–e; Supplementary Figure S3B). In *in vitro* fibrotic models, TGF-β and hypoxia induced the expression of DNMT1, α-SMA, and fibronectin but decreased HOXA5 expression in the mouse kidney proximal tubular BUMPT cells (Supplementary Figure S4).

Collectively, these results indicate that hypermethylation reduces HOXA5 expression in kidney fibrosis.

## Inducible knockout of HOXA5 in proximal tubules aggravates kidney fibrosis in UUO and UIRI

To determine the role of HOXA5 in kidney fibrosis, we established an inducible proximal tubule *Hoxa5* knockout mouse model. To this end, *Hoxa5*-loxp homozygous mice were crossed with *Slc34a1*$^{CreERT2}$ mice[32] to obtain tamoxifen-inducible, proximal-tubule–specific *Hoxa5* knockout mice (Figure 5a). After tamoxifen induction,[33] *Hoxa5*$^{ptCKO}$ mice had significantly lower expression of HOXA5 in kidneys than *Hoxa5*$^{ptCtrl}$ mice (Figure 5b–d; Supplementary Figure S5A). Both UUO and UIRI induced more severe kidney fibrosis in *Hoxa5*$^{ptCKO}$ mice than in *Hoxa5*$^{ptCtrl}$ mice, as indicated by higher levels of collagen deposition (Figure 5e–f; Supplementary Figure S5D and E) and the expression of α-SMA (Figure 5g and i; Supplementary Figure S6F and G), fibronectin (Figure 5h and j; Supplementary Figure S5H), and collagen I (Figure 5k; Supplementary Figure S5I).

To further understand the HOXA5's contribution to renal fibrosis, we performed UUO in *Hoxa5*$^{ptCtrl}$ and *Hoxa5*$^{ptCKO}$ mice with 5-Aza daily injection. 5-Aza significantly decreased the mRNA expression of fibronectin, α-SMA, and collagen I induced by UUO in *Hoxa5*$^{ptCtrl}$ mice but not in *Hoxa5*$^{ptCKO}$ mice (Supplementary Figure S6A–C). In addition, 5-Aza did not reduce collagen deposition induced by UUO in *Hoxa5*$^{ptCKO}$ mice (Supplementary Figure S6D).

These results indicate that loss of HOXA5 in the proximal tubular cells exacerbates kidney fibrogenesis.

## Inducible knockin of HOXA5 in proximal tubules ameliorates renal fibrosis in UUO

To further elucidate the role of HOXA5 in kidney fibrosis, we generated an inducible, proximal-tubule–specific *Hoxa5* knockin (*Hoxa5*$^{ptCKI}$) mouse model (Figure 6a). *Hoxa5*$^{ptCKI}$ mice had significantly higher HOXA5 expression in kidney tissues than wild-type (*Hoxa5*$^{ptWT}$) mice in both sham and UUO conditions (Figure 6b–d; Supplementary Figure S7). Compared with *Hoxa5*$^{ptWT}$ mice, *Hoxa5*$^{ptCKI}$ mice showed less collagen deposition (Figure 6e and f) and less expression of α-SMA (Figure 6g and i), fibronectin (Figure 6h and j), and collagen I (Figure 6k).

## *Jag1* is a potential target of HOXA5 during fibrotic stress in proximal tubular cells

To analyze the mechanism underlying the HOXA5's in kidney fibrosis, we probed its transcriptional targets during TGF-β treatment of renal tubular cells. To this end, normal or HOXA5-overexpressing BUMPT cells were treated with TGF-β for RNA sequencing. TGF-β induced the upregulation of 2147 genes and the downregulation of 2234 genes in normal BUMPT cells. Remarkably, 389 and 458 genes were respectively normalized by HOXA5 overexpression, indicating that these 847 genes were regulated directly or indirectly by HOXA5 in TGF-β-treated renal tubular cells (Figure 7a). We subjected these 847 genes to gene ontology (GO) enrichment analysis leading to 8 GO terms. We found that cluster 6 possessed the largest proportion of "pathway" and "signaling" terms. We chose to analyze

cluster 6 GO terms rather than larger clusters like cluster 1 or 5 because we focused on mechanisms, not phenotypes like “development” or “process” (Figure 7b). We noticed that the NOTCH signaling pathway was ranked in the top 30 pathways in cluster 6 (Figure 7c). Further analysis showed that *Jag1* was significantly induced by TGF-β, and, remarkably, this induction was reduced in HOXA5-overexpressing cells (Figure 7d).

These results suggest that HOXA5 may regulate *Jag1* and associated NOTCH signaling to control fibrosis in kidney tubular cells.

## HOXA5 suppresses JAG1-NOTCH signaling by inhibiting JAG1 expression

We further investigate JAG1 regulation by HOXA5 in kidney fibrosis in mice. JAG1 was barely detectable in sham control kidney proximal tubular cells. After UUO and UIRI, JAG1 was induced in kidney cortex, and more JAG1 expression was observed in $Hoxa5^{ptCKO}$ mice than in $Hoxa5^{ptCtrl}$ mice (Figure 8a and b; Supplementary Figure S8). In contrast, lower JAG1 expression was detected in $Hoxa5^{ptCKI}$ mice than $Hoxa5^{ptWT}$ mice after UUO (Figure 8c and d). As HOXA5 was ablated or overexpressed specifically in kidney proximal tubule cells of transgenic mice, the whole kidney analysis might not represent HOXA5 regulation of *Jag1* in proximal tubule cells. To this end, we isolated kidney proximal tubule cells from these mice for infection with adenovirus-green fluorescent protein or adenovirus-Cre-green fluorescent protein to generate WT, $Hoxa5^{KO}$ cells, or $Hoxa5^{KI}$ cells for comparison (Figure 8e and f). As expected, *Hoxa5* expression was much lower in $Hoxa5^{KO}$ cells and higher in $Hoxa5^{KI}$ cells (Supplementary Figure S9). TGF-β induced *Jag1* mRNA and protein expression in all cells, but the induction was significantly higher in $Hoxa5^{KO}$ tubular cells and significantly lower in $Hoxa5^{KI}$ cells (Figure 8g–j).

$Hoxa5^{KO}$ and WT tubular cells had no differences in *Notch1, Notch2,* and *Notch3* expression during TGF-β treatment (data not shown). However, $Hoxa5^{KO}$ tubular cells had marked higher levels of cleaved NOTCH1, NOTCH2, and NOTCH3 during TGF-β treatment, indicative of NOTCH activation.[34,35] Conversely, NOTCH activation during TGF-β treatment was diminished in $Hoxa5^{KI}$ cells (Figure 8i and j) and in BUMPT cells with HOXA5 overexpression (Supplementary Figure S10A–D). Consistently, the NOTCH effectors *HeyL* and *Hes1* were inhibited after HOXA5 overexpression in BUMPT cells (Supplementary Figure S10E and F) and in UUO tissues with 5-Aza treatment (Supplementary Figure S11A and B).

Collectively, these results indicate that HOXA5 is a negative regulator of JAG1-NOTCH signaling through inhibition of JAG1 expression in kidney fibrosis.

## HOXA5 represses *Jag1* transcription by directly binding to its promoter

To elucidate HOXA5 suppression of JAG1, we performed chromatin immunoprecipitation assays. HOXA5 precipitated with DNA fragments containing motifs 1 and 2, but not motif 3 (Figure 9a and b). The results of a luciferase reporter assay showed that when HOXA5 was introduced, luciferase expression driven by the *Jag1* promoter was repressed compared with control vector transfection (Figure 9c). These findings indicate that HOXA5 represses *Jag1* transcription by directly binding to its promoter.

### HOXA5 is inversely correlated with kidney fibrosis, JAG1, and DNA methylation in kidney biopsies of human CKD patients

Normal kidney biopsy specimens from a nontumor area adjacent to the renal cell carcinoma did not have significant collagen deposition in Masson's trichrome staining, whereas renal biopsies from patients with CKD exhibited obvious collagen deposition or interstitial fibrosis (Figure 10a and b). HOXA5's expression was noticeably reduced in patient samples with CKD (Figure 10c and d) that uncovered a negative correlation between the expression of HOXA5 and kidney fibrosis in human kidney biopsies (Figure 10e). In addition, more JAG1 expression was observed in tubular cells of human CKD kidney tissues than in healthy control. HOXA5 and JAG1 in human kidney biopsies showed a negative correlation in expression patterns (Figure 10f and g).

To support the mechanism that promoter hypermethylation of HOXA5 activates JAG1, we first studied the relationship between HOXA5 and 5mC in human kidneys. Compared with normal tissues, CKD renal biopsies had significantly more 5mC-positive nuclei (Figure 10h and i), which negatively correlated with HOXA5 expression (Figure 10j). We then co-stained 5mC with HOXA5 and 5mC with JAG1. The results showed that HOXA5/5mC co-staining and JAG1/5mC co-staining were more abundant in CKD kidneys than in health controls (Figure 10k and l).

Finally, we analyzed the publicly available datasets to study the promoter methylation of the *HOXA5* gene in human samples of CKD patients and healthy controls. One dataset (GSE50874) included methylation profiling of microdissected human kidney tissues from 21 patients with CKD and 64 healthy controls. The other dataset (GSE230652) provides data on methylation patterns in whole blood samples collected from 93 patients with CKD and 87 healthy controls. The *HOXA5* promoter (chr7:27182613–27185562) was shown to be hypermethylated in kidney tissues of patients with CKD compared with healthy controls (Supplementary Table S9) and in white blood cells from patients with CKD compared with healthy subjects (Supplementary Table S10).

Collectively, human samples indicate that promoter hypermethylation of *HOXA5* is associated with HOXA5 repression, JAG1 activation, and renal fibrosis in CKD, supporting the observations from animal and cellular models in this study.

## DISCUSSION

In the current study, we demonstrate that *Hoxa5* is hypermethylated at its promoter during fibrotic stress, resulting in the repression of *Hoxa5* transcription and expression. Functionally, loss of HOXA5 enhances the expression of JAG1 and, in turn, activates JAG1-NOTCH signaling for renal fibrosis.

The expression of DNMTs and 5mC as well as reduced representation bisulfite sequencing in our study indicates an overall increase of DNA methylation in renal fibrosis during UUO. Consistently, Zeisberg *et al.*[36] detected a significant increase in DNA methylation in fibrotic kidneys after folic acid–induced nephropathy. These studies highlight the potential of demethylating therapies for kidney fibrosis. Nucleotide analogs, such as 5-Aza, are

effective at inhibiting DNMTs, and they are used for treating several types of cancers or malignancies.[37,38] Nevertheless, the clinical use of DNA methylation inhibitors is limited to second-line therapies because they are not gene-specific and have side effects. Thus, it is crucial to determine specific genes with aberrant DNA methylation, explore their biofunctions in diseases, and translate them into clinical applications.

In our present study, we specifically focused on *Hoxa5* because (i) it was hypermethylated at its gene promoter in fibrotic kidneys of mice and patients with CKD and (ii) HOXA5 is a conserved transcriptional factor that regulates the expression of genes involved in kidney injury and repair, such as p53,[39–42] EGR1,[43,44] and b-catenin.[45,46] We show that the hypermethylation of *Hoxa5* in UUO was associated with a marked decrease of its expression, which was prevented by the DNA methylation inhibitor 5-Aza, indicating a critical role of DNA methylation in repressing *Hoxa5* in kidney fibrosis. In the literature, there are scattered reports about the regulation of *Hoxa5* by DNA methylation. For example, Dunn *et al.*[47] detected the hypermethylation of *Hoxa5* in endothelial cells in models of atherosclerosis. Notably, they identified the same 7 hypermethylated CpG sites in the gene promoter of *Hoxa5* as those shown in our sequencing data. Thus, these 7 CpG sites are important to the regulation of *Hoxa5* expression by DNA methylation and may serve as specific therapeutic targets. In this regard, our study has demonstrated the first evidence for a role of HOXA5 in renal fibrosis. Especially, we show that specific knockout of HOXA5 in kidney proximal tubules aggravated, whereas knockin of HOXA5 alleviated, renal fibrosis in mice. These observations indicate that DNA hypermethylation leads to the repression of HOXA5, contributing to renal fibrogenesis. In addition to DNA methylation, HOXA5 may be subjected to regulation by other mechanisms, including miRNAs, long noncoding RNAs, and histone acetylation.[21,22] Future research needs to determine the contributions of these mechanisms to HOXA5 regulation in kidney fibrosis.

*Hoxa5* is a member of the homeobox genes, which encode a family of transcription factors involved in patterning in the early stages of embryonic development.[21,22] Aberrant *Hoxa* gene expression has been implicated in diseases, especially in various types of cancers.[22] However, the downstream target genes of HOXA5 remain largely unknown. In the present study, we analyzed the target genes of HOXA5 in proximal tubular cells under fibrotic stress by RNA sequencing, showing a few fibrosis-associated genes regulated by HOXA5, including *Fn1, Timp1*,[48,49] *Timp3*,[50,51] *Jag1*,[52,53] *Hes1*,[52] *Aspn*,[54,55] and *Tet1*.[56] The RNA sequencing results in combination with further bioinformatics analysis suggested *Jag1* as a key target of HOXA5. Indeed, the chromatin immunoprecipitation assay detected the binding of HOXA5 to the promoter sequence of *Jag1*, and the regulation of *Jag1* promoter activity by HOXA5 was verified by a luciferase reporter assay. We further verified that the knockout of HOXA5 increased JAG1 expression in proximal tubular cells of the kidney, whereas knockin of HOXA5 had opposite effects. JAG1 is a critical ligand of the NOTCH signaling pathway, which plays an important role in fibrotic kidney diseases.[52,53,57] Notably, JAG1 is also the most abundant NOTCH ligand expressed in human and mouse kidneys. Also, among these ligands, the expression of JAG1 is most strongly correlated with kidney fibrosis. JAG1 is normally expressed in the distal tubule and collecting duct cells, but, in fibrotic condition, it is induced on the basal and lateral membrane in proximal tubular cells.[52,53] The role of JAG1 in renal fibrosis was convincingly demonstrated by using kidney

tubule–specific *Jag1* knockout mice.[53] When *Jag1* in tubular epithelial cells was deleted, NOTCH signaling was suppressed and kidney fibrosis alleviated.[53] By demonstrating the regulation of *Jag1* by HOXA5, our current work significantly advances the understanding of the upstream mechanism of NOTCH signaling in kidney fibrosis.

Our work may also provide an explanation for the sustained NOTCH activation observed in kidney fibrosis.[53] As an epigenetic mechanism, DNA methylation is inheritable. Accordingly, hypermethylation of *Hoxa5* in kidney fibrosis is a stable modification that would be inherited during cell division. As a consequence, HOXA5 remains to be down-regulated, and JAG1 is continuously activated for persistent NOTCH activation. These observations suggest novel therapeutic strategies for fibrotic kidney disease by blocking DNA methylation on the 7 CpG sites in the *Hoxa5* gene promoter.

## Supplementary Material

Refer to Web version on PubMed Central for supplementary material.

## ACKNOWLEDGMENTS

This work was supported in part by the grants from the National Institutes of Health (DK058831 and DK087843) of the USA and the Department of Veterans Administration of the USA (BX000319) to ZD, and the grants from the National Natural Science Foundation of China (81500513 and 82170704) and Natural Science Foundation of Hubei Province (2022CFB218) to XX. ZD is a recipient of The Senior Research Career Scientist award from the Department of Veterans Affairs of United States.

## DATA STATEMENT

The raw data of reduced representation bisulfite sequencing were stored in the GEO datasets (GSE: GSE246417). RNA sequencing data in this research are available in SRA with BioProject accession number PRJNA979014 (https://www.ncbi.nlm.nih.gov/sra/PRJNA979014).

## REFERENCES

1. Liyanage T, Toyama T, Hockham C, et al. Prevalence of chronic kidney disease in Asia: a systematic review and analysis. BMJ Glob Health. 2022;7:e007525.
2. Kalantar-Zadeh K, Jafar TH, Nitsch D, et al. Chronic kidney disease. Lancet. 2021;398:786–802. [PubMed: 34175022]
3. Lau WL, Fisher M. New insights into cognitive decline in chronic kidney disease. Nat Rev Nephrol. 2023;19:214–215. [PubMed: 36460897]
4. Azizan EAB, Drake WM, Brown MJ. Primary aldosteronism: molecular medicine meets public health. Nat Rev Nephrol. 2023;19:788–806. [PubMed: 37612380]
5. Humphreys BD. Mechanisms of renal fibrosis. Annu Rev Physiol. 2018;80:309–326. [PubMed: 29068765]
6. Li L, Fu H, Liu Y. The fibrogenic niche in kidney fibrosis: components and mechanisms. Nat Rev Nephrol. 2022;18:545–557. [PubMed: 35788561]
7. Guo C, Dong G, Liang X, Dong Z. Epigenetic regulation in AKI and kidney repair: mechanisms and therapeutic implications. Nat Rev Nephrol. 2019;15:220–239. [PubMed: 30651611]
8. Bergmann C, Distler JH. Epigenetic factors as drivers of fibrosis in systemic sclerosis. Epigenomics. 2017;9:463–477. [PubMed: 28343418]

9. Zhang Q, Yin S, Liu L, et al. Rhein reversal of DNA hypermethylation-associated Klotho suppression ameliorates renal fibrosis in mice. Sci Rep. 2016;6:34597. [PubMed: 27703201]
10. Xiao C, Gao L, Hou Y, et al. Chromatin-remodelling factor Brg1 regulates myocardial proliferation and regeneration in zebrafish. Nat Commun. 2016;7:13787. [PubMed: 27929112]
11. Zhang L, Zhang Q, Liu S, et al. DNA methyltransferase 1 may be a therapy target for attenuating diabetic nephropathy and podocyte injury. Kidney Int. 2017;92:140–153. Kidney Int 2018;93:271. [PubMed: 28318634]
12. Kato M, Natarajan R. Epigenetics and epigenomics in diabetic kidney disease and metabolic memory. Nat Rev Nephrol. 2019;15:327–345. [PubMed: 30894700]
13. Liu P, Liu Y, Liu H, et al. Role of DNA de novo (de)methylation in the kidney in salt-induced hypertension. Hypertension. 2018;72:1160–1171. [PubMed: 30354815]
14. Agodi A, Barchitta M, Maugeri A, et al. Unveiling the role of DNA methylation in kidney transplantation: novel perspectives toward biomarker identification. Biomed Res Int. 2019;2019:1602539.
15. Zhu B, Poeta ML, Costantini M, et al. The genomic and epigenomic evolutionary history of papillary renal cell carcinomas. Nat Commun. 2020;11:3096. [PubMed: 32555180]
16. Kumar P, Brooks HL. Sex-specific epigenetic programming in renal fibrosis and inflammation. Am J Physiol Renal Physiol. 2023;325:F578–F594. [PubMed: 37560775]
17. Bechtel W, McGoohan S, Zeisberg EM, et al. Methylation determines fibroblast activation and fibrogenesis in the kidney. Nat Med. 2010;16:544–550. [PubMed: 20418885]
18. Yin S, Zhang Q, Yang J, et al. TGFbeta-incurred epigenetic aberrations of miRNA and DNA methyltransferase suppress Klotho and potentiate renal fibrosis. Biochim Biophys Acta Mol Cell Res. 2017;1864:1207–1216. [PubMed: 28285987]
19. Tampe B, Tampe D, Zeisberg EM, et al. Induction of Tet3-dependent epigenetic remodeling by low-dose hydralazine attenuates progression of chronic kidney disease. EBioMedicine. 2015;2:19–36. [PubMed: 25717475]
20. Vervaet BA, Moonen L, Godderis L, et al. Untargeted DNA-demethylation therapy neither prevents nor attenuates ischemia-reperfusion-induced renal fibrosis. Nephron. 2017;137:124–136. [PubMed: 28750405]
21. Jeannotte L, Gotti F, Landry-Truchon K. Hoxa5: a key player in development and disease. J Dev Biol. 2016;4:13. [PubMed: 29615582]
22. Fan F, Mo H, Zhang H, et al. HOXA5: a crucial transcriptional factor in cancer and a potential therapeutic target. Biomed Pharmacother. 2022;155:113800.
23. Yoo KH, Park YK, Kim HS, et al. Epigenetic inactivation of HOXA5 and MSH2 gene in clear cell renal cell carcinoma. Pathol Int. 2010;60:661–666. [PubMed: 20846263]
24. den Dekker HT, Burrows K, Felix JF, et al. Newborn DNA-methylation, childhood lung function, and the risks of asthma and COPD across the life course. Eur Respir J. 2019;53:1801795.
25. Dressler GR. The cellular basis of kidney development. Annu Rev Cell Dev Biol. 2006;22:509–529. [PubMed: 16822174]
26. Edeling M, Ragi G, Huang S, et al. Developmental signalling pathways in renal fibrosis: the roles of Notch, Wnt and Hedgehog. Nat Rev Nephrol. 2016;12:426–439. [PubMed: 27140856]
27. Cao Z, Lis R, Ginsberg M, et al. Targeting of the pulmonary capillary vascular niche promotes lung alveolar repair and ameliorates fibrosis. Nat Med. 2016;22:154–162. [PubMed: 26779814]
28. Li J, Dong S, Ye M, et al. MicroRNA-489–3p represses hepatic stellate cells activation by negatively regulating the JAG1/Notch3 signaling pathway. Dig Dis Sci. 2021;66:143–150. [PubMed: 32144602]
29. Nemir M, Metrich M, Plaisance I, et al. The Notch pathway controls fibrotic and regenerative repair in the adult heart. Eur Heart J. 2014;35:2174–2185. [PubMed: 23166366]
30. Cheng JX, Chen L, Li Y, et al. RNA cytosine methylation and methyltransferases mediate chromatin organization and 5-azacytidine response and resistance in leukaemia. Nat Commun. 2018;9:1163. [PubMed: 29563491]

31. Ko YA, Mohtat D, Suzuki M, et al. Cytosine methylation changes in enhancer regions of core pro-fibrotic genes characterize kidney fibrosis development. Genome Biol. 2013;14:R108. [PubMed: 24098934]
32. Kusaba T, Lalli M, Kramann R, et al. Differentiated kidney epithelial cells repair injured proximal tubule. Proc Natl Acad Sci U S A. 2014;111:1527–1532. [PubMed: 24127583]
33. Liu T, Yuan J, Dai C, et al. Cre/loxP approach-mediated downregulation of Pik3c3 inhibits the hypertrophic growth of renal proximal tubule cells. J Cell Physiol. 2020;235:9958–9973. [PubMed: 32474911]
34. Jarriault S, Brou C, Logeat F, et al. Signalling downstream of activated mammalian Notch. Nature. 1995;377:355–358. [PubMed: 7566092]
35. Kopan R, Ilagan MX. The canonical Notch signaling pathway: unfolding the activation mechanism. Cell. 2009;137:216–233. [PubMed: 19379690]
36. Zeisberg EM, Zeisberg M. The role of promoter hypermethylation in fibroblast activation and fibrogenesis. J Pathol. 2013;229:264–273. [PubMed: 23097091]
37. Xu X, Tan X, Tampe B, et al. High-fidelity CRISPR/Cas9-based gene-specific hydroxymethylation rescues gene expression and attenuates renal fibrosis. Nat Commun. 2018;9:3509. [PubMed: 30158531]
38. Short NJ, Kantarjian H. Hypomethylating agents for the treatment of myelodysplastic syndromes and acute myeloid leukemia: past discoveries and future directions. Am J Hematol. 2022;97:1616–1626. [PubMed: 35871436]
39. Raman V, Martensen SA, Reisman D, et al. Compromised HOXA5 function can limit p53 expression in human breast tumours. Nature. 2000;405:974–978. [PubMed: 10879542]
40. Ma Z, Li L, Livingston MJ, et al. p53/microRNA-214/ULK1 axis impairs renal tubular autophagy in diabetic kidney disease. J Clin Invest. 2020;130:5011–5026. [PubMed: 32804155]
41. Cao JY, Wang B, Tang TT, et al. Exosomal miR-125b-5p deriving from mesenchymal stem cells promotes tubular repair by suppression of p53 in ischemic acute kidney injury. Theranostics. 2021;11:5248–5266. [PubMed: 33859745]
42. Zhang D, Liu Y, Wei Q, et al. Tubular p53 regulates multiple genes to mediate AKI. J Am Soc Nephrol. 2014;25:2278–2289. [PubMed: 24700871]
43. Ai K, Li X, Zhang P, et al. Genetic or siRNA inhibition of MBD2 attenuates the UUO- and I/R-induced renal fibrosis via downregulation of EGR1. Mol Ther Nucleic Acids. 2022;28:77–86. [PubMed: 35356685]
44. Chen H, Rubin E, Zhang H, et al. Identification of transcriptional targets of HOXA5. J Biol Chem. 2005;280:19373–19380. [PubMed: 15757903]
45. Zhang H, Zhao JH, Suo ZM. Knockdown of HOXA5 inhibits the tumorigenesis in esophageal squamous cell cancer. Biomed Pharmacother. 2017;86:149–154. [PubMed: 27960137]
46. Tan RJ, Zhou D, Zhou L, Liu Y. Wnt/beta-catenin signaling and kidney fibrosis. Kidney Int Suppl (2011). 2014;4:84–90. [PubMed: 26312156]
47. Dunn J, Qiu H, Kim S, et al. Flow-dependent epigenetic DNA methylation regulates endothelial gene expression and atherosclerosis. J Clin Invest. 2014;124:3187–3199. [PubMed: 24865430]
48. Barmada A, Klein J, Ramaswamy A, et al. Cytokinopathy with aberrant cytotoxic lymphocytes and profibrotic myeloid response in SARS-CoV-2 mRNA vaccine-associated myocarditis. Sci Immunol. 2023;8:eadh3455.
49. Dwivedi N, Jamadar A, Mathew S, et al. Myofibroblast depletion reduces kidney cyst growth and fibrosis in autosomal dominant polycystic kidney disease. Kidney Int. 2023;103:144–155. [PubMed: 36273656]
50. Wang Y, Yue S, Cai F, et al. Treatment of berberine alleviates diabetic nephropathy by reducing iron overload and inhibiting oxidative stress. Histol Histopathol. 2023;38:1009–1016. [PubMed: 36861878]
51. Alex L, Tuleta I, Hanna A, et al. Diabetes induces cardiac fibroblast activation, promoting a matrix-preserving nonmyofibroblast phenotype, without stimulating pericyte to fibroblast conversion. J Am Heart Assoc. 2023;12:e027463.
52. Bielesz B, Sirin Y, Si H, et al. Epithelial Notch signaling regulates interstitial fibrosis development in the kidneys of mice and humans. J Clin Invest. 2010;120:4040–4054. [PubMed: 20978353]

53. Huang S, Park J, Qiu C, et al. Jagged1/Notch2 controls kidney fibrosis via Tfam-mediated metabolic reprogramming. PLoS Biol. 2018;16:e2005233.

54. Huang C, Sharma A, Thakur R, et al. Asporin, an extracellular matrix protein, is a beneficial regulator of cardiac remodeling. Matrix Biol. 2022;110:40–59. [PubMed: 35470068]

55. Liu L, Yu H, Long Y, et al. Asporin inhibits collagen matrix-mediated intercellular mechanocommunications between fibroblasts during keloid progression. FASEB J. 2021;35:e21705.

56. Gu Y, Chen J, Zhang H, et al. Hydrogen sulfide attenuates renal fibrosis by inducing TET-dependent DNA demethylation on Klotho promoter. FASEB J. 2020;34:11474–11487. [PubMed: 32729950]

57. Djudjaj S, Chatziantoniou C, Raffetseder U, et al. Notch-3 receptor activation drives inflammation and fibrosis following tubulointerstitial kidney injury. J Pathol. 2012;228:286–299. [PubMed: 22806125]

## Translational Statement

DNA methylation has been implicated in kidney fibrosis. In this study, we demonstrated the induction of DNA methyltransferases and global DNA methylation in fibrotic kidneys and further proved the beneficial effects of their inhibitor 5-Aza in renal fibrosis. HOXA5 was shown to be downregulated in fibrotic kidneys through hypermethylation, and this downregulation led to JAG1 expression and consequent activation of NOTCH signaling for kidney fibrogenesis. These findings unveil DNA methylation and related genes, such as *HOXA5*, as potential therapeutic targets in kidney fibrotic disease.

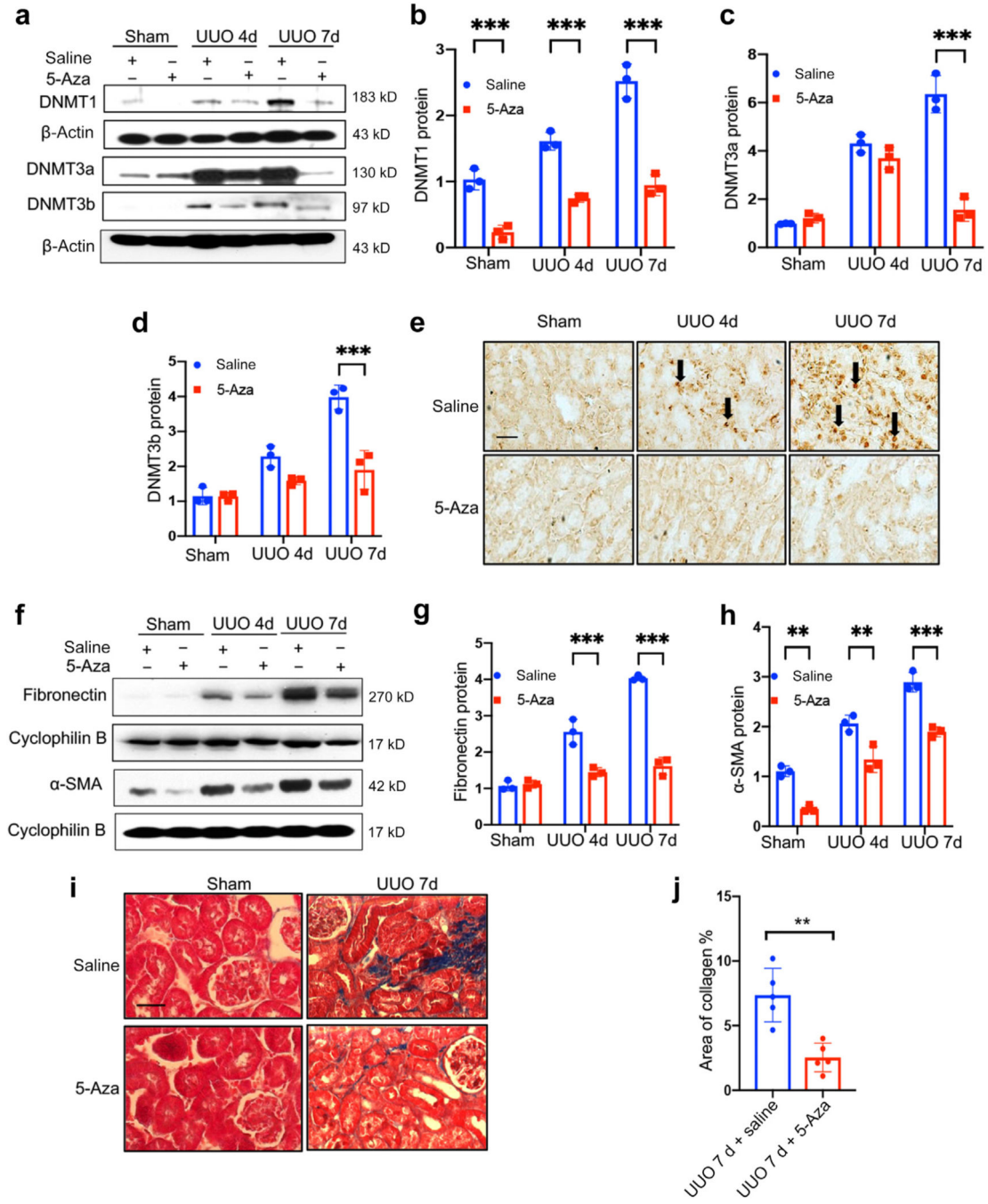


**Figure 1 |. DNA methylation are induced in kidney during unilateral ureter obstruction (UUO) and pharmacological inhibition of DNA methylation suppresses renal fibrosis.**

C57BL/6 mice were subjected to UUO and then injected daily with 1 mg/kg body weight of 5-Aza or the same volume of saline for 4 or 7 days. (**a**) Immunoblots showing the induction of DNA methyltransferases (DNMT1, DNMT3a, and DNMT3b) in kidney cortex tissues during UUO and the inhibitory effects of 5-Aza. (**b–d**) Densitometry of DNMT1, DNMT3a, and DNMT3b protein expression (n = 3 per group). (**e**) Immunohistochemistry of 5mC showing UUO-induced DNA methylation in kidneys and the inhibitory effects of

5-Aza. (**f**) Immunoblots showing the expression of fibronectin and α-SMA in UUO kidney tissues and the inhibitory effects of 5-Aza. (**g,h**) Densitometry of fibronectin and α-SMA on immunoblots (n = 3 per group). (**i**) Masson's trichrome staining of renal fibrosis in UUO kidneys and the inhibitory effects of 5-Aza. Bar = 20 μm. (**j**) Quantification of Masson's trichrome staining signals with Image J (n = 5). Panels (**b–d**) and (**g,h**) were analyzed using 1-way analysis of variance, and panel (**j**) was analyzed with a 2-tailed Student's *t* test. **P* < 0.05, ***P* < 0.01, ****P* < 0.001. 5mC, 5′-methylcytosine; α-SMA, α-smooth muscle actin. To optimize viewing of this image, please see the online version of this article at www.kidney-international.org.

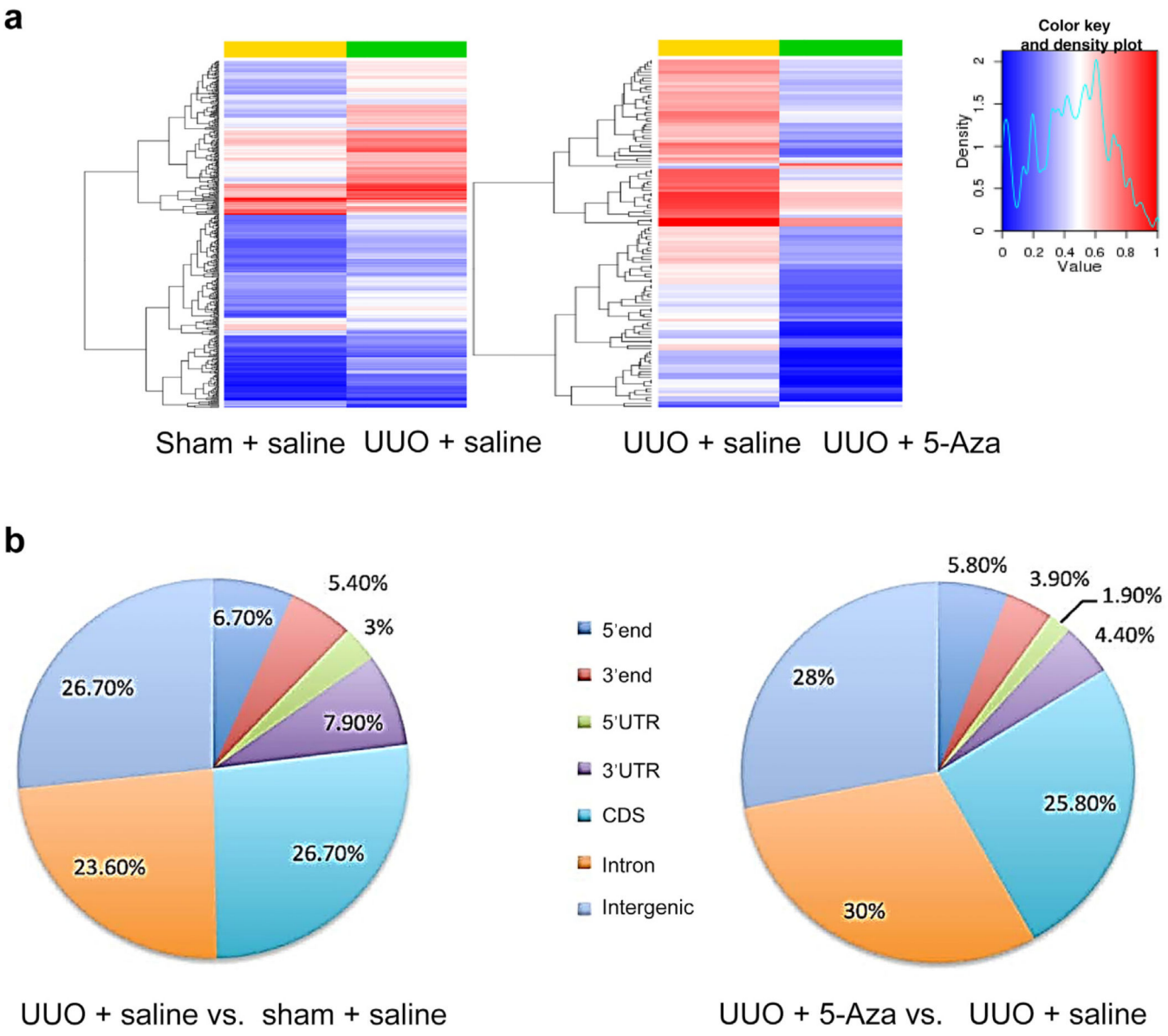


**Figure 2 |. Profiling of DNA methylation in unilateral ureter obstruction (UUO) kidneys.**

C57BL/6 mice were divided into 3 groups: sham surgery with daily saline injection, UUO for 7 days with daily saline, and UUO for 7 days with daily 5-Aza injection (n = 2 for each group). Kidney cortex tissue was collected to isolate genomic DNA for global DNA methylation analysis with reduced representation bisulfite sequencing. (**a**) Heatmaps of differentially methylated regions (DMRs). The average value of methylation percentage from 2 mice was calculated to represent the methylation level for each CpG site, and DMRs were the windows (non-overlapping sequences of 200 nucleotides) with significant differences of methylation between the experimental groups. The redder: the higher level of DNA methylation; the bluer: the lower level of DNA methylation. (**b**) Distribution of DMRs induced by UUO and the effect of 5-Aza. CDS, coding sequence; UTR, untranslated region.

**a**

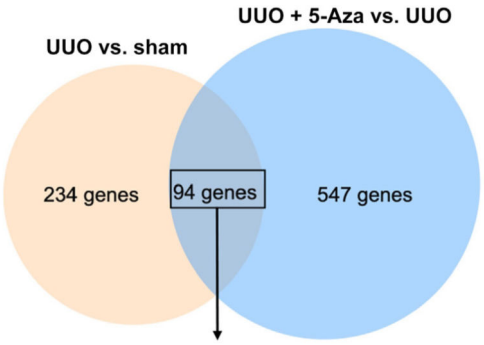


**Genes with promoter hypermethylation during UUO and hypomethylation by treating with UUO and 5-Aza**

| Location | Start | End | Gene name | DMR sites |
|---|---|---|---|---|
| chr2 | 17961201 | 17961400 | *A930004D18Rik* | 5'end |
| chr2 | 32597801 | 32598000 | *6330409D20Rik* | 5'end |
| chr5 | 151476301 | 151476500 | *Pds5b* | 5'UTR1, 5'end, exon1 |
| chr6 | 52154701 | 52154900 | *Hoxa5* | 5'end |
| chr7 | 31098901 | 31099100 | *AI428936* | 5'end |

**b**

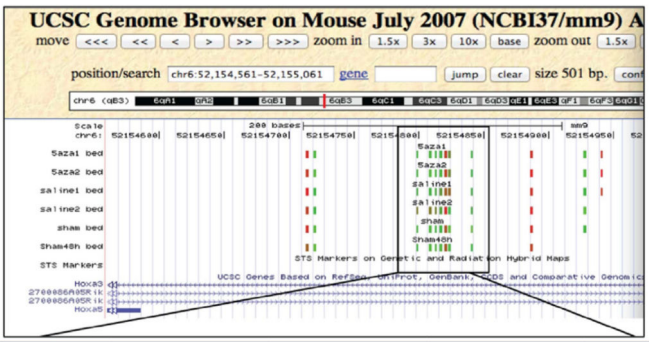


**c**

| | Site | 1 | 2 | 3 | 4 | 5 | 6 | 7 |
|---|---|---|---|---|---|---|---|---|
| RRBS | Sham | 15.75% | 10.30% | 11.95% | 16.05% | 66.75% | 7.15% | 10.70% |
| | UUO+saline | 42.30% | 41.35% | 40.40% | 38.70% | 73.75% | 42.50% | 32.55% |
| | UUO+5-Aza | 15.95% | 9.20% | 18.85% | 17.65% | 75.60% | 46.10% | 22.90% |

**d**

| | Site | 1 | 2 | 3 | 4 | 5 | 6 | 7 |
|---|---|---|---|---|---|---|---|---|
| Pyrosequencing | Sham | 65.57% | 73.25% | 59.83% | 40.57% | 54.06% | 58.65% | 61.89% |
| | UUO+saline | 88.08% | 98.50% | 77.23% | 49.82% | 71.42% | 75.20% | 91.55% |
| | UUO+5-Aza | 71.11% | 80.16% | 62.09% | 39.89% | 54.19% | 58.60% | 67.38% |

**Figure 3 |. Promoter methylation of *Hoxa5* gene is associated with renal fibrosis in unilateral ureter obstruction (UUO).**

(**a**) UUO induced hypermethylation in 234 genes compared with sham control, and 5-Aza led to the hypomethylation of 547 genes during UUO. There were 94 genes that had hypermethylation in UUO that were normalized by 5-Aza. In these 94 genes, 5 had methylation changes in their promoter region, including *A930004D18Rik*, *6330409D20Rik*, *Pds5b*, *Hoxa5*, and *AI428936*. (**b**) University of California, Santa Cruz (UCSC) genome browser screenshot showing a differentially methylated region with 7 CpG sites in the

gene promoter region of *Hoxa5* (chr6:52154700–52154850, mm9). (**c**) UUO-induced increase of DNA methylation at each CpG site and the inhibitory effect of 5-Aza in reduced representation bisulfite sequencing (RRBS) analysis. (**d**) Promoter region of *Hoxa5* (chr6:52154700–52154850, mm9) was subjected to pyrosequencing. The percentage of DNA 5′-methylcytosine (5mC) methylation was calculated for each CpG site in sham control, UUO+saline, and UUO+5-Aza groups. UUO significantly induced DNA hypermethylation in *Hoxa5*'s promoter (*P* value was 0.0130) and 5-Aza inhibited the promoter methylation (*P* value 0.0149 tested by 1-way analysis of variance).

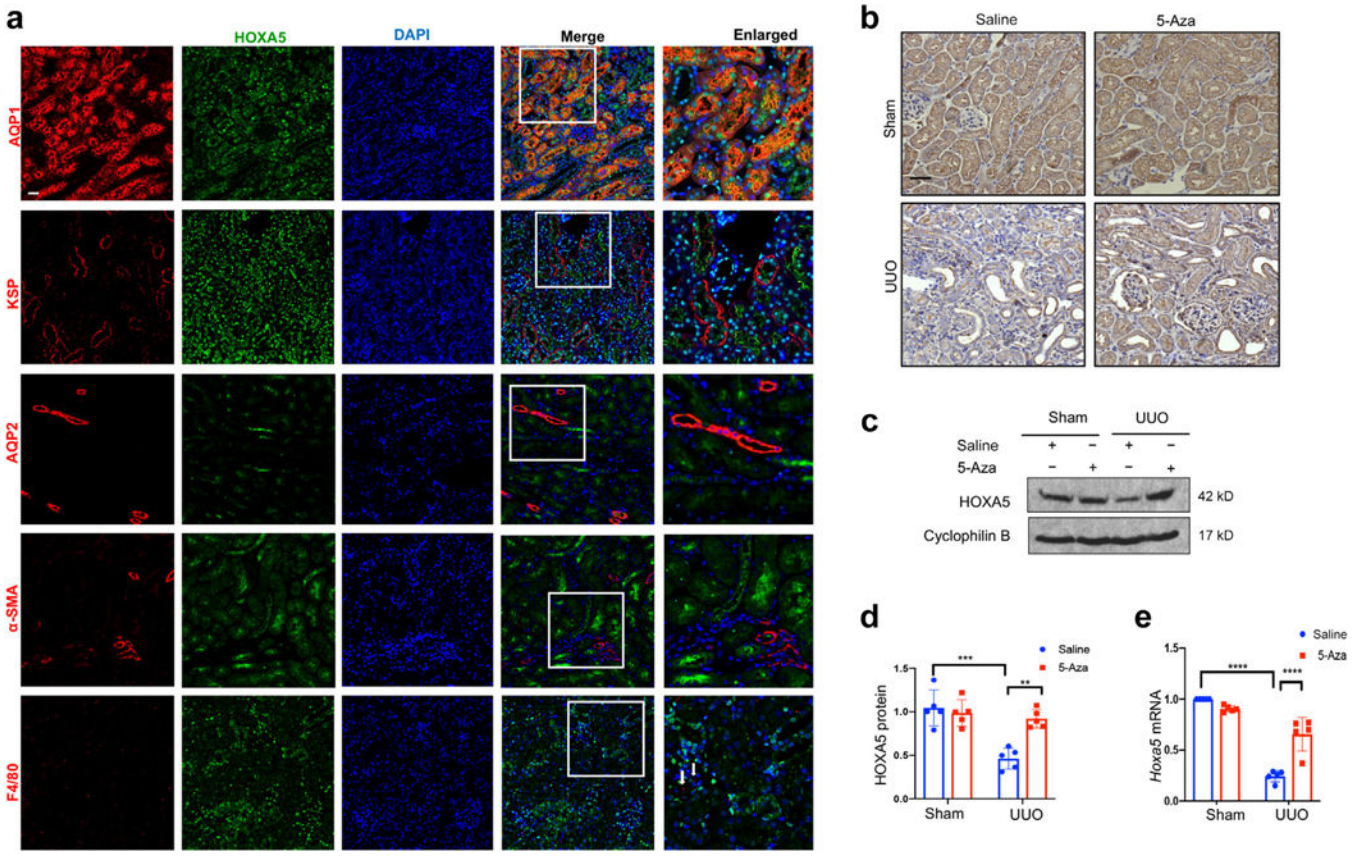


**Figure 4 |. HOXA5 is expressed in tubular cells and its expression is regulated by DNA methylation.**

(**a**) Immunofluorescence of HOXA5 (green) and renal tubule markers (red) along with 4′,6-diamidino-2-phenylindole (DAPI) staining of nuclei (blue) in normal mouse kidneys. Aquaporin 1 (AQP1), kidney-specific cadherin-positive (KSP), and aquaporin 2 (AQP2) are specific markers of proximal tubule, distal tubule, and collecting tubule, respectively. α-smooth muscle actin (α-SMA) and F4/80 are markers of myofibroblasts and macrophages, respectively. The enlarged panels on the right side show higher magnification images of the boxed regions. (**b**) C57BL/6 mice were subjected to α-smooth muscle actin (UUO) for 7 days or sham operation, and then injected with saline or 5-Aza to collect kidney tissues. Immunohistochemical staining showing that UUO induced HOXA5 decrease, which was prevented by 5-Aza. Bar = 20 μm. (**c**) Representative immunoblots showing the HOXA5 decrease in UUO kidneys and the inhibitory effect of 5-Aza treatment. (**d**) Densitometry of HOXA5 bands in blots (n = 5). (**e**) Kidney cortical tissues were analyzed for relative levels of *Hoxa5* mRNA by real-time polymerase chain reaction (n = 5). Panels (**d**) and (**e**) were analyzed using 2-way analysis of variance. $^{**}P < 0.01$, $^{***}P < 0.001$, and $^{****}P < 0.0001$. To optimize viewing of this image, please see the online version of this article at www.kidney-international.org.

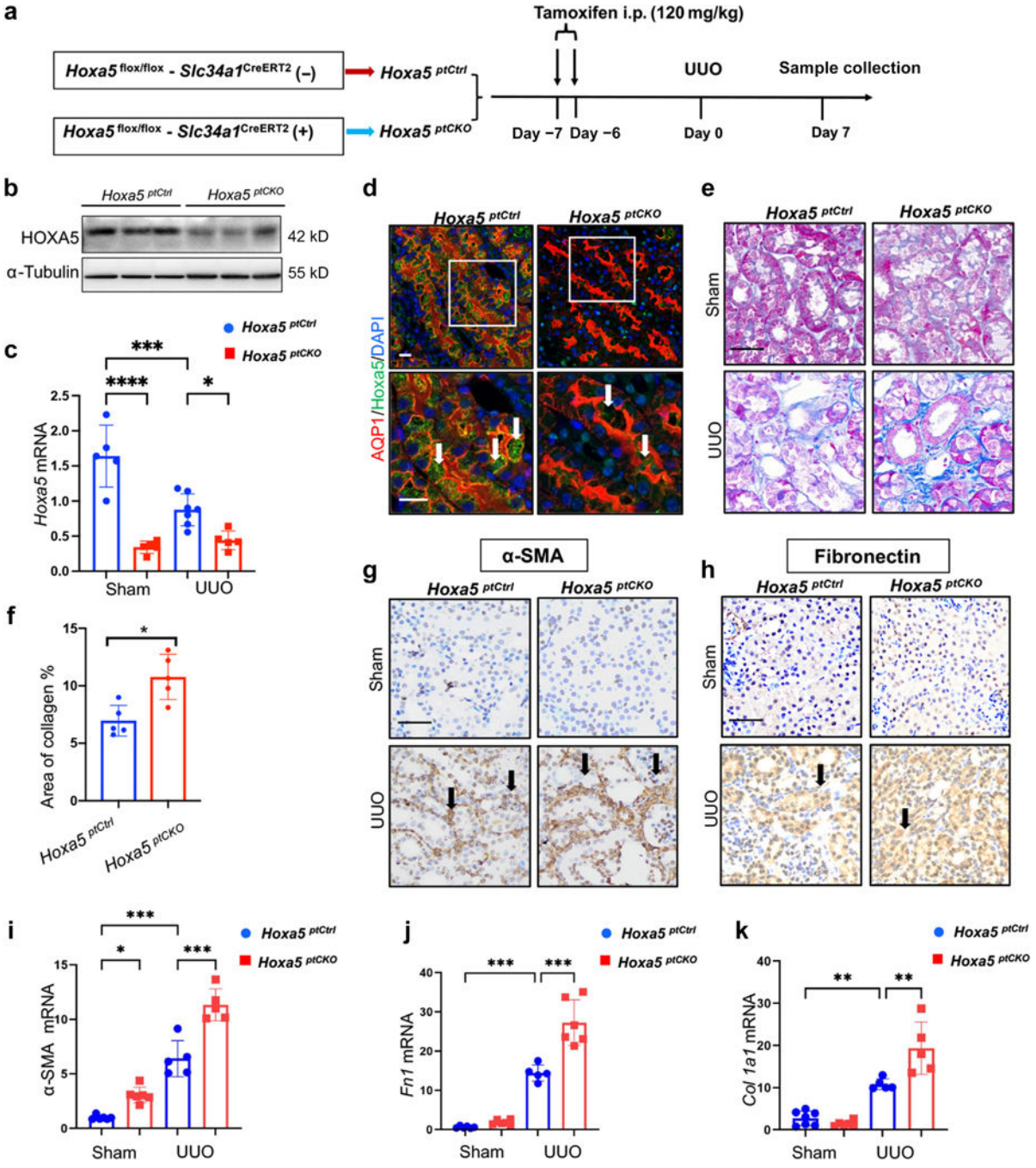


**Figure 5 |. Inducible knockout of HOXA5 in proximal tubules aggravates renal fibrosis in unilateral ureter obstruction (UUO).**

(**a**) Experimental design: *Hoxa5*$^{ptCKO}$ mice and *Hoxa5*$^{ptCtrl}$ control littermates were given 120 mg/kg tamoxifen (i.p.) at 7 and 6 days before UUO to induce HOXA5 ablation from kidney proximal tubules in *Hoxa5*$^{ptCKO}$ mice but not in *Hoxa5*$^{ptCtrl}$ mice. The mice were then subjected to UUO or sham operation. Kidneys were collected 7 days later. (**b**) Representative immunoblots showing significant less HOXA5 in *Hoxa5*$^{ptCKO}$ mice kidneys than in *Hoxa5*$^{ptCtrl}$. (**c**) Reverse transcription-quantitative polymerase chain reaction

analysis of mRNA verifying *Hoxa5* ablation in kidneys of $Hoxa5^{ptCKO}$ mice in comparison with $Hoxa5^{ptCtrl}$ kidneys (n = 5–9 per group). (**d**) Double immunofluorescence staining of HOXA5 (green) and aquaporin 1 (AQP1; red) to show the effect of proximal tubule–specific knockout of HOXA5. (**e**) Representative Masson's trichrome staining of kidney tissues. Bar = 20 μm. (**f**) Quantitative analysis of Masson's trichrome staining of kidney sections (n = 5). Immunohistochemical staining of α-smooth muscle actin (α-SMA) (**g**) and fibronectin (**h**) showing more fibrotic protein staining (black arrow) in $Hoxa5^{ptCKO}$ kidneys after UUO. Bar = 20 μm. (**i–k**) Higher levels of α-SMA (**i**), fibronectin (**j**), and collagen I (**k**) mRNAs in the kidneys of $Hoxa5^{ptCKO}$ mice than that of $Hoxa5^{ptCtrl}$ mice (n = 5–6 per group). Panels (**c**) and (**i–k**) were analyzed using 1-way analysis of variance, and panel (**f**) was analyzed with a 2-tailed Student's *t* test. $*P < 0.05$, $**P < 0.01$, and $****P < 0.0001$. DAPI, 4′,6-diamidino-2-phenylindole. To optimize viewing of this image, please see the online version of this article at www.kidney-international.org.

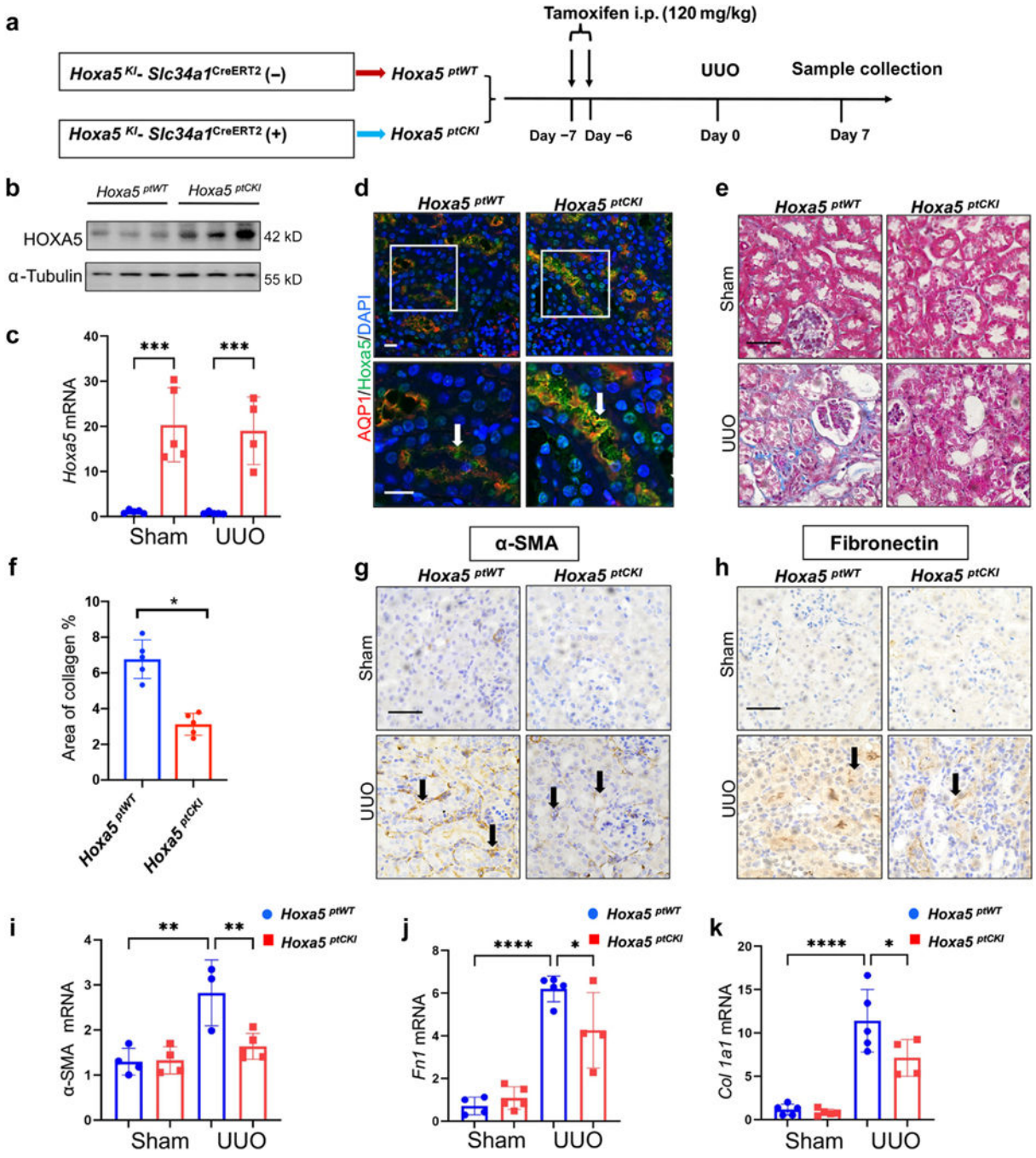


**Figure 6 |. Inducible knockin of HOXA5 in proximal tubules ameliorates renal fibrosis in unilateral ureter obstruction (UUO).**

(**a**) Experimental design: *Hoxa5*$^{ptCKI}$ mice and *Hoxa5*$^{ptWT}$ littermates were given 120 mg/kg tamoxifen (i.p.) at 7 and 6 days before UUO to induce HOXA5 overexpression in kidney proximal tubules in *Hoxa5*$^{ptCKI}$ mice but not in *Hoxa5*$^{ptWT}$ mice. The mice were then subjected to UUO or sham operation to collect kidneys 7 days later. (**b**) Immunoblot analysis showing HOXA5 overexpression in kidney tissues of *Hoxa5*$^{ptCKI}$ mice in comparison with *Hoxa5*$^{ptWT}$ mice. (**c**) Reverse transcription-quantitative polymerase chain reaction

analysis of mRNA confirming elevated levels of *Hoxa5* transcripts in the kidneys of $Hoxa5^{ptCKI}$ mice compared with $Hoxa5^{ptWT}$ mice (n = 5). (**d**) Coimmunofluorescence of HOXA5 and aquaporin 1 (AQP1) showing specific HOXA5 overexpression in proximal tubules. (**e**) Representative Masson's trichrome staining of kidney tissues. Bar = 20 μm. (**f**) Quantitative analysis of Masson's trichrome staining of kidney sections (n = 5). (**g,h**) Immunohistochemical staining of α-SMA (**g**) and fibronectin (**h**) showing less fibrotic proteins (black arrow) in $Hoxa5^{ptCKI}$ kidneys after UUO. Bar = 20 μm. (**i–k**) mRNA levels of α-smooth muscle actin (α-SMA) (**i**), fibronectin (**j**), and collagen I (**k**) in kidneys of $Hoxa5^{ptWT}$ and $Hoxa5^{ptCKI}$ mice (n = 3–5 per group). Panels (**c**) and (**i–k**) were analyzed using 1-way analysis of variance, and panel (**f**) was analyzed with a 2-tailed Student's *t* test. $*P < 0.05$, $**P < 0.01$, and $****P < 0.0001$. To optimize viewing of this image, please see the online version of this article at www.kidney-international.org.

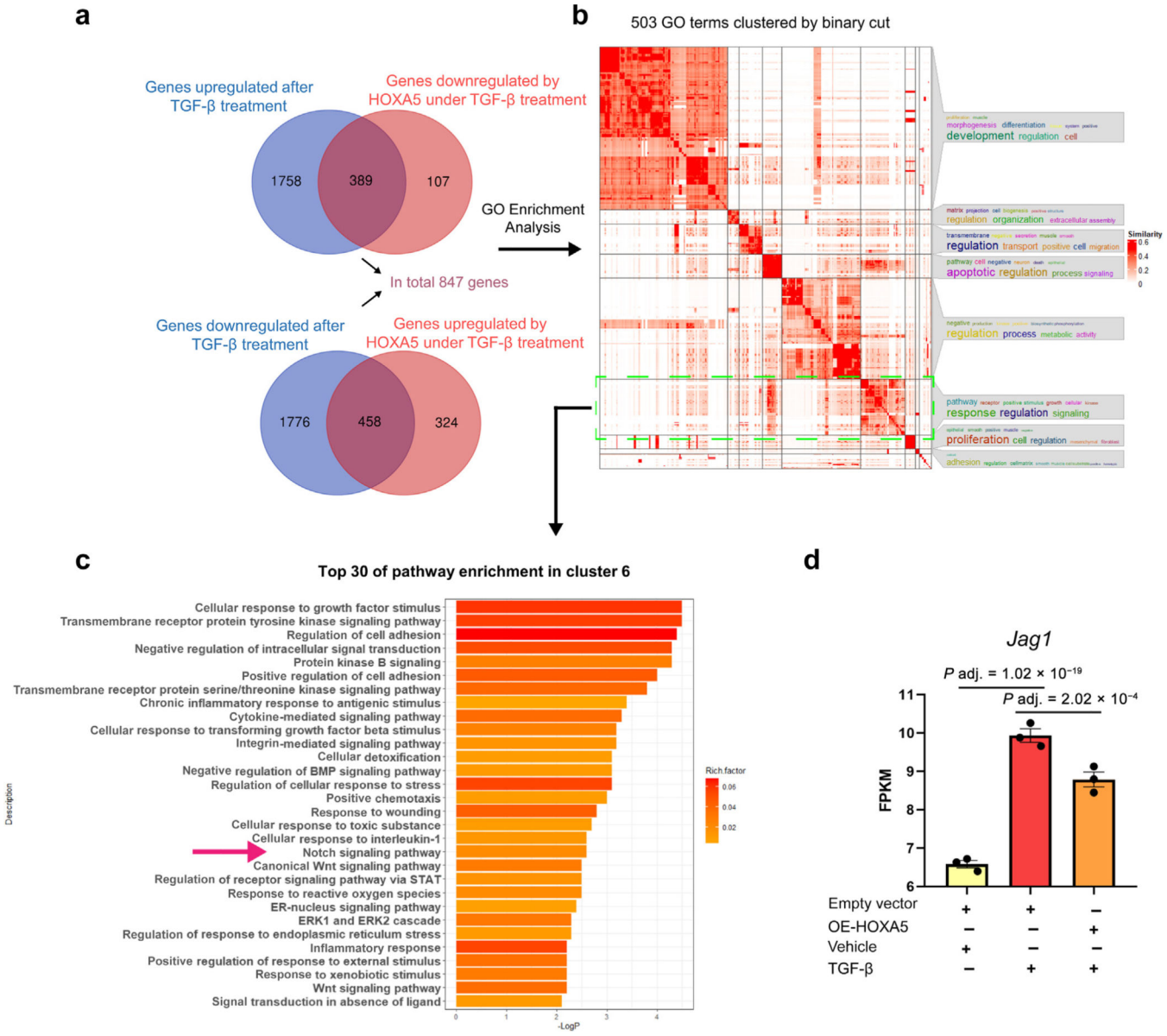


**Figure 7 |. *Jag1* is a potential target of HOXA5 during fibrotic stress in proximal tubular cells.** (**a**) BUMPT cells transfected with pcDNA3.1-*Hoxa5* or control vector were treated with 10 ng/ml of transforming growth factor-β (TGF-β) for 48 hours to collect samples for RNA sequencing. In control vector-transfected cells, TGF-β induced the upregulation of 2147 (1758 + 389) genes, of which 389 were attenuated in *Hoxa5*-transfected cells. TGF-β also induced the downregulation of 2234 (1776 + 458) genes, of which the downregulation of 458 was prevented in *Hoxa5*-transfected cells. (**b**) The 847 (389 + 458) genes affected by HOXA5 during TGF-β treatment were selected for the gene ontology (GO) enrichment analysis. The 503 significant terms of the GO enrichment were classified into 8 main clusters by cola and simplify enrichment. (**c**) Top 30 of the signaling pathways in cluster 6 including the NOTCH signaling pathway. (**d**) Inhibition of *Jag1* expression during TGF-β treatment by HOXA5. The level of *Jag1* transcripts was represented by

Fragments Per Kilobase of exon model per Million mapped fragment (FPKM). BMP, bone morphogenetic protein; ER, endoplasmic reticulum; ERK, extracellular signal–regulated kinase; OE, overexpress; STAT, signal transducer and activator of transcription.

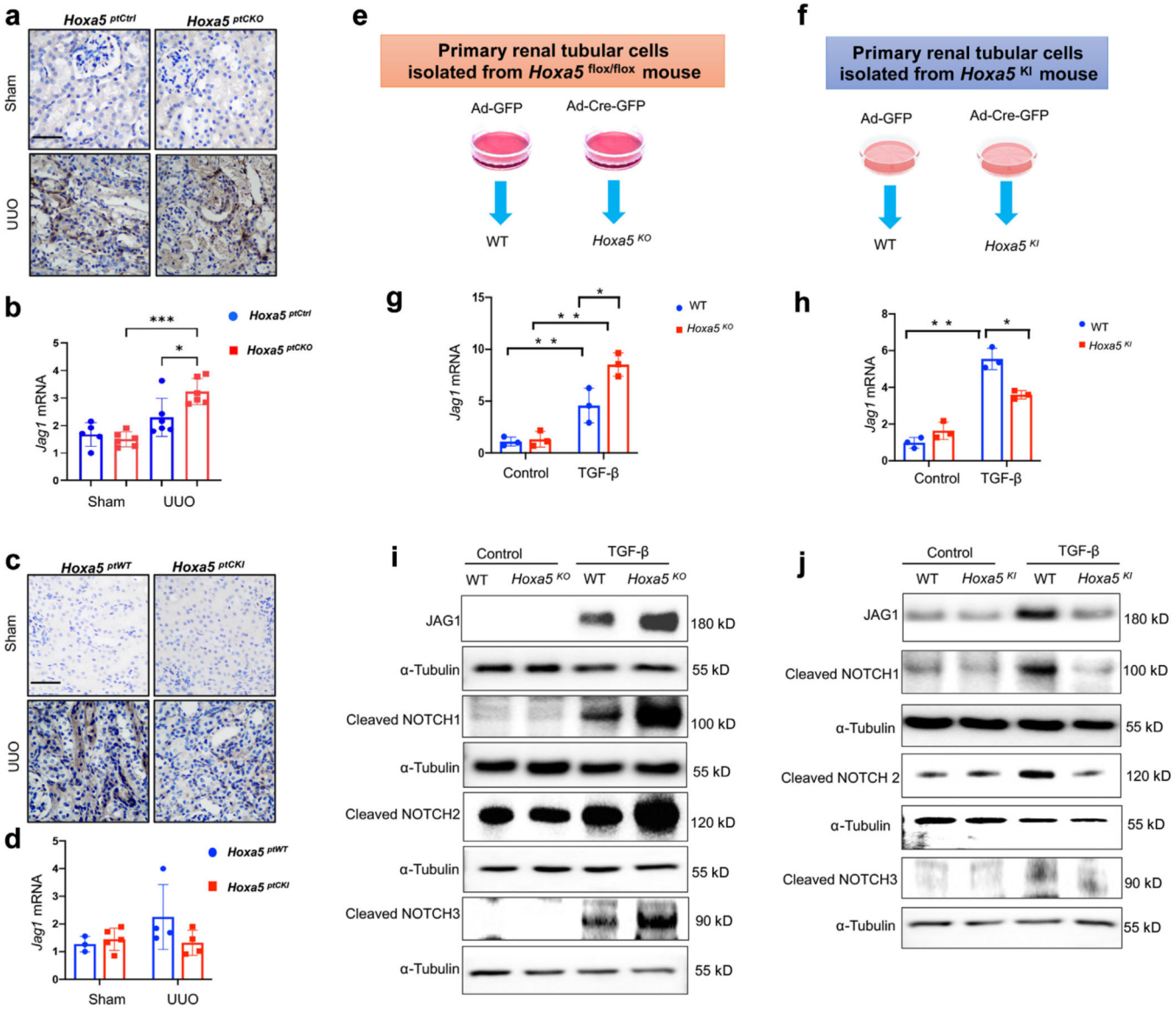


**Figure 8 |. HOXA5 suppresses JAG1-NOTCH signaling by inhibiting JAG1 expression in mice.**

(**a**) Immunohistochemical staining showing more JAG1 staining in *Hoxa5*$^{ptCKO}$ mouse kidney tubules than in *Hoxa5*$^{ptCtrl}$ after unilateral ureter obstruction (UUO). Bar = 20 μm. (**b**) Reverse transcription-quantitative polymerase chain reaction analysis detected a higher *Jag1* mRNA level in *Hoxa5*$^{ptCKO}$ mouse kidneys than in *Hoxa5*$^{ptCtrl}$ kidneys after UUO (n = 4–6 mice per group). (**c**) Immunohistochemical staining showing less JAG1 staining in *Hoxa5*$^{ptCKI}$ mouse kidney tubules than in *Hoxa5*$^{ptWT}$ after UUO. Bar = 20 μm. (**d**) RT-qPCR analysis showing a lower level of *Jag1* mRNA in *Hoxa5*$^{ptCKI}$ mouse kidneys than in *Hoxa5*$^{ptWT}$ kidneys (n = 5 mice per group). (**e**) Primary kidney tubular cells isolated from *Hoxa5*-loxp homozygous mice were infected with adenovirus carrying the Cre expressing sequence (Ad-Cre-GFP) or the control virus (Ad-GFP). (**f**) Primary kidney tubular cells isolated from *Hoxa5*-knockin homozygous mice were infected with adenovirus carrying the Cre expressing sequence (Ad-Cre-GFP) or the control virus (Ad-GFP). (**g**)

Transforming growth factor-β (TGF-β) treatment for 72 hours induced more *Jag1* mRNA in *Hoxa5*$^{KO}$ tubular cells than in wild type (WT) cells. (**h**) *Jag1* mRNA induction by 72 hours of TGF-β treatment was suppressed in *Hoxa5*$^{KI}$ tubular cells in comparison to WT cells. (**i**) Representative immunoblots showing higher induction of JAG1, cleaved NOTCH1, cleaved NOTCH2, and cleaved NOTCH3 by TGF-β in *Hoxa5*$^{KO}$ primary tubular cells and in WT cells. (**j**) Immunoblots showing lower induction of JAG1, cleaved NOTCH1, cleaved NOTCH2, and cleaved NOTCH3 by TGF-β in *Hoxa5*$^{KI}$ primary tubular cells than in WT tubular cells. Panels (**g**) and (**h**) were analyzed using 1-way analysis of variance, $*P < 0.05$, $**P < 0.01$, and $****P < 0.0001$. To optimize viewing of this image, please see the online version of this article at www.kidney-international.org.

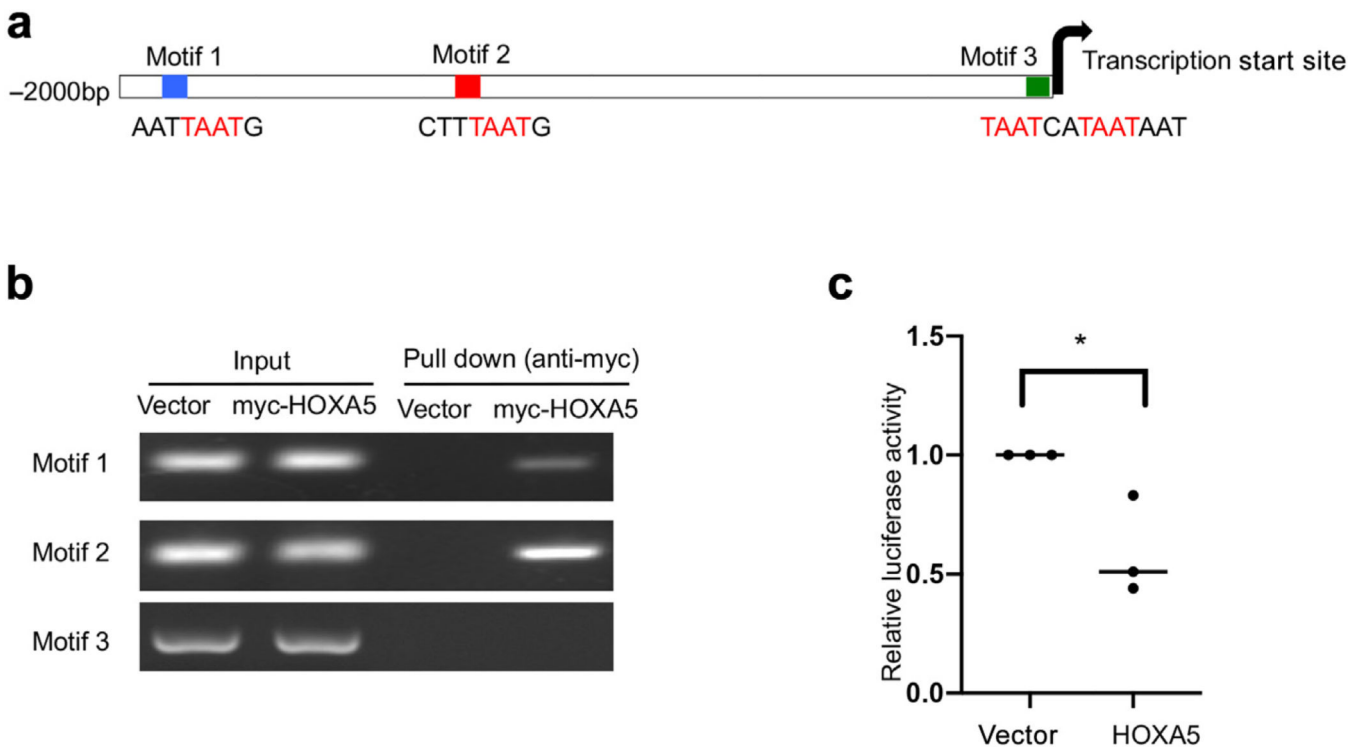


**Figure 9 |. HOXA5 represses *Jag1* transcription by directly binding to its promoter.**

(**a**) Locations and sequences of the 3 predicted Hoxa5-binding motifs in the promoter region of Jag1. (**b**) Chromatin immunoprecipitation assay showing the binding of HOXA5 to 2 predicted binding motifs in the promoter region of Jag1. BUMPT cells were transfected with pcDNA-3.1-*myc-his-Hoxa5* plasmid or empty vector. Anti-myc antibody was used to pull down myc-his-HOXA5 and associated DNAs for PCR amplification using specific primer pairs, which showed the binding of HOXA5 to motifs 1 and 2, but not motif 3, of the *Jag1* promoter. (**c**) HEK293 cells were co-transfected with the luciferase reporter gene containing *JAG1* promoter sequences, pGL3 control plasmid, and pcDNA-3.1-myc-his-*HOXA5* plasmid or empty vector. Luciferase activity was measured at 48 hours after transfection to show the inhibitory effect of HOXA5 on *JAG1* promoter activity (n = 3). Data were analyzed with a 2-tailed Student's *t* test. **P* < 0.05. PCR, polymerase chain reaction.

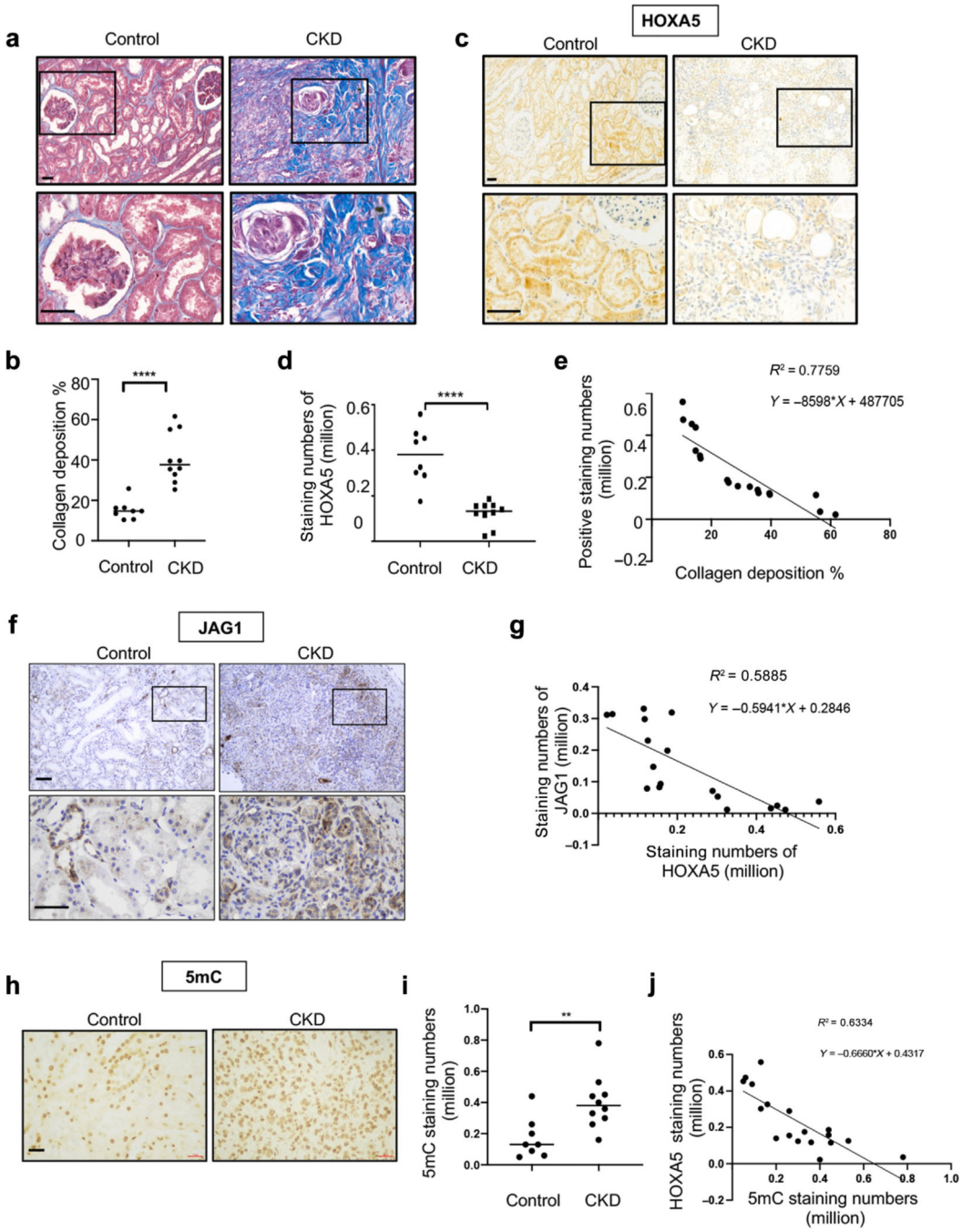

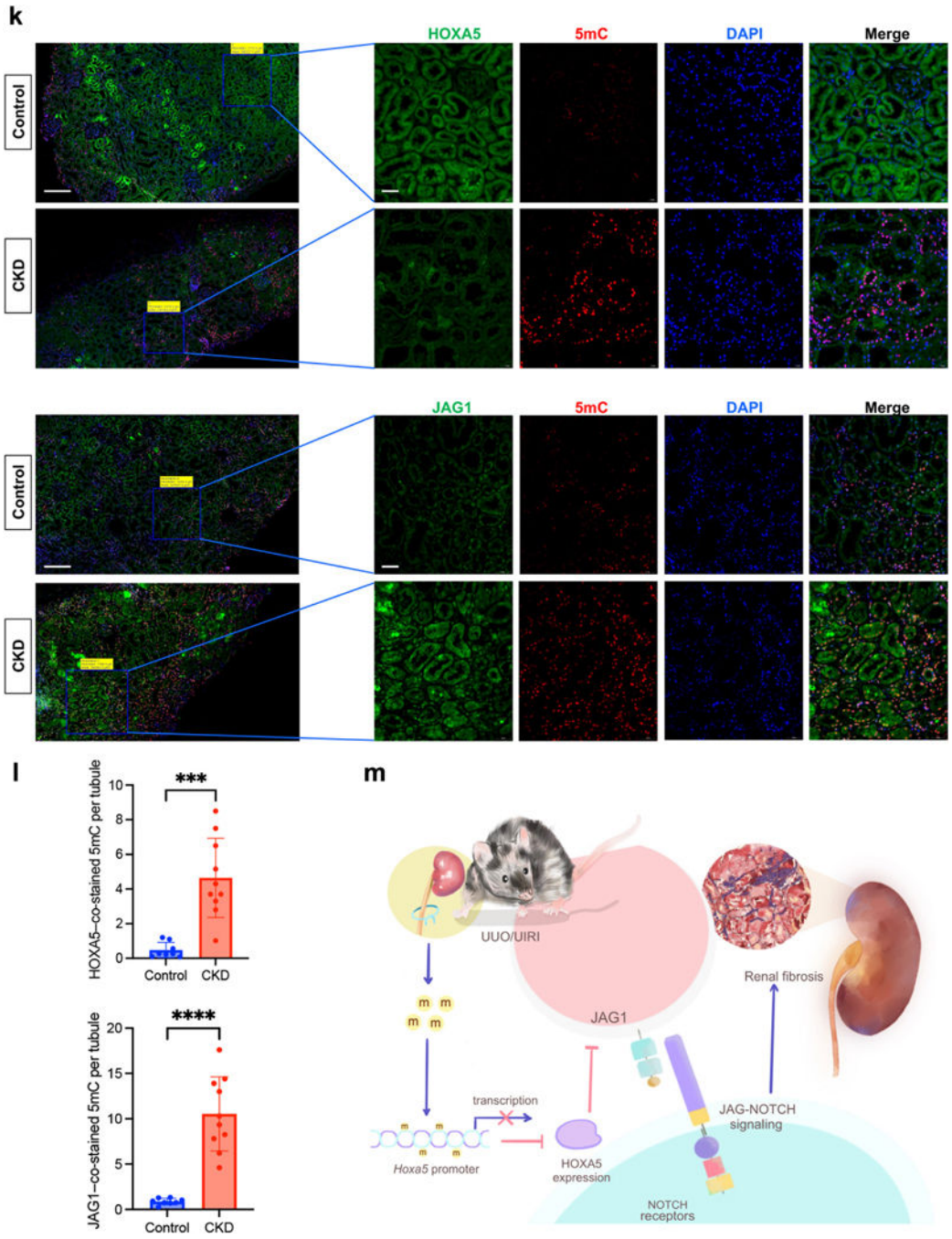


**Figure 10 |. HOXA5 is inversely correlated with renal fibrosis, JAG1, and DNA methylation in renal biopsies of human patients with chronic kidney disease (CKD).**

(**a**) Masson's trichrome staining of renal biopsies from patients with CKD (CKD group) (n = 10) and normal paracarcinoma tissues of patients with renal cancer (control group) (n = 8). The lower panels are higher magnification images of the boxed areas in the upper panels. Bar = 10 μm. (**b**) Quantification of collagen deposition (Masson's trichrome staining positive) in normal paracarcinoma kidney tissues (control, n = 8) and the CKD group of human biopsies (CKD, n = 10). (**c**) Immunohistochemical staining of HOXA5

in CKD biopsies and paracarcinoma kidney tissues (control). The lower panels are higher magnification images of the boxed areas in the upper panels. Bar = 10 μm. (**d**) Quantification of HOXA5 staining in control and CKD kidney tissues (control group: n = 8, CKD group: n = 10). (**e**) Correlation of HOXA5 staining with collagen deposition in human renal tissues (n = 18). (**f**) Immunohistochemical staining of JAG1 in control and CKD kidney tissues. Bar = 10 μm. (**g**) Correlation of HOXA5 staining with JAG1 staining in human renal tissues (n = 18). (**h**) Immunohistochemical staining of 5mC in control and CKD kidney tissues. Bar = 10 μm. (**i**) Quantification of 5mC staining in control and CKD biopsies (control group: n = 8, CKD group: n = 10). (**j**) Correlation of HOXA5 staining and 5mC staining in human renal tissues (n = 18). (**k**) Representative image for co-staining of 5′-methylcytosine (5mC; red) and HOXA5 (green) or JAG1 (green) by immunofluorescence staining in control and CKD kidney tissues. Bar = 200 μm for original scanned image (cropped) and 50 μm for enlarged images. (**l**) Quantification of HOXA5–co-stained 5mC and JAG1–co-stained 5mC (control group: n = 8, CKD group: n = 10). (**m**) Proposed mechanism of HOXA5 in renal fibrosis. Panels (**b,d,i,l**) were analyzed with a 2-tailed Student's *t* test. $*P < 0.05$. Panels (**e**), (**g**), and (**j**) were analyzed with linear regression (*P* values for each were less than 0.001). To optimize viewing of this image, please see the online version of this article at www.kidney-international.org.